Field-tuned quantum critical point of antiferromagnetic metals

I. Fischer and A. Rosch
Institut für Theoretische Physik, Universität zu Köln, 50937 Köln, Germany
(Received 13 December 2004; published 31 May 2005)

A magnetic field applied to a three-dimensional antiferromagnetic metal can destroy the long-range order and thereby induce a quantum critical point. Such field-induced quantum critical behavior has been the focus of many recent experiments. We theoretically investigate the quantum critical behavior of clean antiferromagnetic metals subject to a static, spatially uniform, external magnetic field. The external field not only suppresses (or induces in some systems) antiferromagnetism, but also influences the dynamics of the order parameter by inducing spin precession. This leads to an exactly *marginal* correction to spin-fluctuation theory. We investigate how the interplay of precession and damping determines the specific heat, magnetization, magnetocaloric effect, susceptibility, and scattering rates. We point out that precession can change the sign of the leading $\sqrt{T}$ correction to the specific-heat coefficient $c(T)/T$ and can induce a characteristic maximum in $c(T)/T$ for certain parameters. We argue that the susceptibility $\chi=\partial M/\partial B$ is the thermodynamic quantity that shows the most significant change upon approaching the quantum critical point, and which gives experimental access to the (dangerously irrelevant) spin-spin interactions.

DOI: 10.1103/PhysRevB.71.184429 PACS number(s): 73.43.Nq, 75.40.−s, 71.10.Hf, 75.30.Sg

The study of quantum phase transitions is currently a very active field of research in theoretical as well as experimental condensed-matter physics. Particularly in a large number of metals—mostly heavy Fermion or transition-metal compounds—the critical fluctuations associated with a quantum phase transition induce anomalous behavior in thermodynamic and transport quantities such as diverging specific-heat coefficients or a linear resistivity quite distinct from the behavior of a conventional Fermi liquid.

Experimentally, there are three main methods to use in tuning a system towards a quantum critical point: doping, pressure, and magnetic field. Doping has the disadvantage that it induces disorder, and it cannot be easily adjusted within a single sample. These problems are absent if pressure is used as the control parameter of the quantum phase transitions. However, the presence of a pressure cell makes many experiments difficult. For this reason, many recent experiments[1–12] investigate field-tuned quantum critical behavior, where an external magnetic field is used to control the distance from the quantum critical point. Generally it is expected that the presence of a magnetic field changes the universality class of the transition, as in its presence time-reversal invariance is broken. In this paper, we will therefore theoretically analyze the quantum critical behavior of a clean, itinerant antiferromagnet in three dimensions, subject to a static, spatially uniform, external magnetic field B.

Such a situation has been investigated in a number of experiments.[1–6] For example, in $CeCu_{5.2}Ag_{0.8}$ (Ref. 1) and $CeCu_{5.8}Au_{0.2}$ (Ref. 2) magnetic order can be suppressed by moderate magnetic fields. In these systems the quantum critical behavior induced by a magnetic field B appears to be qualitatively different, compared to the critical properties for vanishing field (controlled by pressure or doping). In the presence of a field these systems seem to follow[1] the predictions from spin-fluctuation theory[13–15] for three-dimensional nearly antiferromagnetic metals. This is not the case for $B=0$,[16] where other scenarios have been proposed.[17] Similarly experiments[3] in field-tuned $YbCu_{5-x}Al_x$ appear to be consistent with spin-fluctuation theory, which is not found to be the case in $YbRh_2Si_2$, where magnetic order is suppressed by tiny magnetic fields.[4] Recently, in $CeCoIn_5$ (Refs. 7 and 8) the superconducting order was suppressed by a magnetic field—it is at the moment a controversial question whether the observed anomalous behavior is related to a superconducting quantum critical point or whether magnetism plays a role in this system.

Another interesting class of systems is *insulators* such as $TlCuCl_3$,[9] $SrCu_2(BO_3)_2$,[10] or $BaCuSi_2O_6$,[11] where antiferromagnetic order has been *induced* by the application of a magnetic field B. These transitions[9] can be interpreted as a Bose-Einstein condensation (see below) of spin-1 excitations. The energy of the "spin-up" component of such triplets is lowered by B until it condenses at a critical field, $B=B_c$, thereby inducing an antiferromagnetic order perpendicular to the magnetic field.

In contrast to classical transitions, the dynamics, i.e., the temporal quantum fluctuations, of the order parameter determines the nature and universality class of a quantum phase transition. For example, at the critical point of an insulating antiferromagnet, the dynamics of the order parameter Φ can be described[18] as in a Klein-Gordon equation $(\partial_t^2-\boldsymbol{\nabla}^2)\Phi$. In such a system, typical frequencies ω scale linearly with the momentum $\omega\propto q^z$ where $z=1$ is the dynamical, critical exponent. In contrast, in a metal the excitation of particle-hole pairs leads to a Landau damping[14] of the antiferromagnetic order parameter $(\partial_t+\boldsymbol{\nabla}^2)\Phi$, and therefore $z=2$. Here we assumed that the ordering vector $\boldsymbol{Q}$ is sufficiently small, $Q<2k_F$, such that low-energy particle-hole pairs with momentum $\boldsymbol{Q}$ exist.

A magnetic field will have two main effects: first it will suppress (or in some cases[5] also induce) magnetic order. More interesting is the second effects, it induces a precession

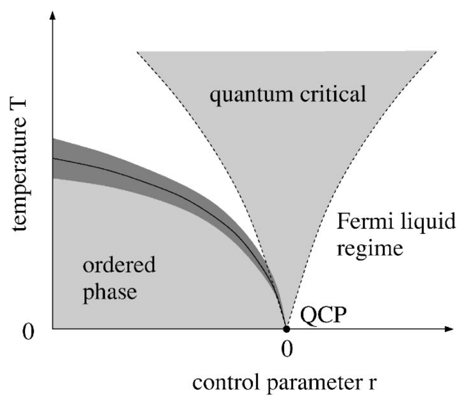

FIG. 1. Schematic phase diagram of a quantum phase transition with a control parameter $r \propto B - B_c$.

of the magnetic moments $\boldsymbol{S}$ perpendicular to the magnetic field,

$$\partial_t \boldsymbol{S} = \boldsymbol{B} \times \boldsymbol{S}, \tag{1}$$

and therefore modifies the dynamics of the order parameter. The linear time derivative also translates to a dynamical exponent $z=2$, and therefore arises the question of how the precession competes with damping in a metal that is characterized by the same z. For insulating systems the physics of the precession term has been widely discussed.[18–23] The corresponding quantum critical behavior as a function of the magnetic field of such an insulating magnet in an external field is actually well known: it is expected to be in the same universality class as the quantum phase transition of a low-density interacting Bose-Einstein condensate as a function of chemical potential. The linear time derivative $i\partial_t \Psi$ of the Schrödinger equation can in this case be identified with the precession term (1) (see below).

In the following, we study the interplay of ohmic damping and spin precession terms in the case of a nearly antiferromagnetic metal. First we present the model for the order-parameter field and a short derivation of the effective action. Then we list the renormalization-group equations for the parameters of the model and use them to derive the behavior of the correlation length. In the following sections we calculate the specific heat, thermal expansion, magnetocaloric effect, and susceptibility. We show for example that sufficiently large magnetic fields can induce sign changes in the critical contribution to the specific heat, and that the susceptibility is particularly suited to probe the vicinity of the quantum critical point. Finally, we investigate the influence of the B field on the scattering rate of the electrons.

I. MODEL AND EFFECTIVE ACTION

Following Hertz,[14] we describe the critical behavior of an antiferromagnetic metal entirely in terms of the effective Ginzburg-Landau-Wilson theory of an order-parameter field $\boldsymbol{\Phi}(\boldsymbol{r},t)$ that represents the fluctuating (staggered) magnetization of the system.

In the absence of a magnetic field, the quadratic part of the action takes the form[14] (assuming negligible spin-orbit coupling),

$$S_2'[\boldsymbol{\Phi}] = \frac{1}{\beta} \int \frac{d^3k}{(2\pi)^3} \sum_n \boldsymbol{\Phi}^*(r + k^2 + |\omega_n|)\boldsymbol{\Phi}, \tag{2}$$

where r measures the distance from the quantum critical point, and momenta $\boldsymbol{k}$ are given relative to the antiferromagnetic-ordering wave vector $\boldsymbol{Q}$. The $|\omega_n|$ term arises from the (Landau-) damping of the spin fluctuations by gapless fermionic excitations in the vicinity of points on the Fermi surface that are connected by $\boldsymbol{Q}$ (assuming $Q < 2k_F$).

How will this effective action change in the presence of a magnetic field? First, $r=r(B)$ will acquire a magnetic-field dependence. For example, r will grow for larger fields in systems where antiferromagnetism is suppressed by B. Second, the magnetic field breaks the rotational invariance and components of Φ parallel, and perpendicular to $\boldsymbol{B}$ will have different masses, r_z and $r_\perp$, respectively. Third, as argued above, the magnetization will precess around $\boldsymbol{B}$; this is described by an extra term (in coordinate and time space for convenience),

$$\begin{aligned} S_2^{pr}[\boldsymbol{\Phi}] &= \int_0^\beta d\tau \int d\mathbf{r} \boldsymbol{b} \cdot \mathrm{i}(\boldsymbol{\Phi} \times \partial_t \boldsymbol{\Phi}) \\ &= \int \int b(\mathrm{i}\Phi_x \partial_t \Phi_y - \mathrm{i}\Phi_y \partial_t \Phi_x) \\ &= \int \int b \tilde{\Phi}_\perp^* \partial_t \tilde{\Phi}_\perp, \end{aligned} \tag{3}$$

in the effective action, where $\boldsymbol{b}$ is parallel to $\boldsymbol{B}$ (taken to point into the $\hat{z}$ direction), and we have introduced the complex field $\tilde{\Phi}_\perp = \Phi_x + \mathrm{i}\Phi_y$. Note that (3) breaks time-reversal invariance. Therefore such a term is absent for $\boldsymbol{B}=0$.

Above, we deduced the form of the effective action on phenomenological grounds, but it can also be derived from a more explicit calculation, starting from a Hubbard-type model of electrons moving in the presence of a magnetic field, $H = \Sigma_{\boldsymbol{k}\sigma}(\epsilon_{\boldsymbol{k}} + B\sigma^z_{\sigma\sigma})\psi^\dagger_{\boldsymbol{k}\sigma}\psi_{\boldsymbol{k}\sigma} + U\Sigma n_\downarrow n_\uparrow$. Here, the magnetic field enters only via a Zeeman term; we do not take orbital effects into account, assuming that Landau levels are broadened by disorder or thermal effects. Note that in the experimentally most relevant heavy Fermion system, orbital effects are strongly suppressed, compared to contributions from the Zeeman term as the effective masses and magnetic susceptibilities are very large in those systems.[24]

For simplicity, we assume that the antiferromagnet is commensurate (incommensurate antiferromagnets show the same qualitative behavior for all quantities discussed below) and introduce a real order-parameter vector $\boldsymbol{\Phi}(\boldsymbol{x},t)$ as a Hubbard-Stratonovich field that decouples the spin-density part of the interaction. Following Hertz, the electrons are now integrated out to obtain an effective action for the order parameter, generating *a priori* infinitely many interaction terms. We truncate the effective action, retaining the leading frequency and momentum dependence of the Gaussian part of the action as well as a constant $\boldsymbol{\Phi}$ (Ref. 4) interaction term, since all other terms are irrelevant in the renormalization group sense[14,15] (cubic terms are discussed in Appendix A). For the quadratic part one obtains $S_2 = (1/\beta)\Sigma_{\omega,\boldsymbol{k}}\Phi^{\alpha}_{\omega_n,\boldsymbol{k}}[\delta_{\alpha\alpha'}/J+\chi^0_{\alpha\alpha'}(\boldsymbol{k},\mathrm{i}\omega_n)]\Phi^{\alpha'}_{-\omega_n,-\boldsymbol{k}}$ where J is the interaction in the spin-spin channel, and $\chi^0_{\alpha\alpha'}(\mathbf{k},i\omega_n)$ is the susceptibility in the presence of the finite field $\boldsymbol{B}$ evaluated at $J=0$. Calculating these susceptibilities on the paramagnetic side of the transition we obtain

$$S = S_2[\boldsymbol{\Phi}] + S_4[\boldsymbol{\Phi}],$$

$$S_2[\boldsymbol{\Phi}] = \frac{1}{\beta}\int \frac{d^3k}{(2\pi)^3}\sum_n \boldsymbol{\Phi}^T_{\omega_n,\boldsymbol{k}}\begin{pmatrix} r_\perp + |\omega_n|\cos\theta + k^2 & \omega_n \sin\theta & 0 \\ -\omega_n\sin\theta & r_\perp + |\omega_n|\cos\theta + k^2 & 0 \\ 0 & 0 & r_z + |\omega_n| + k^2 \end{pmatrix}\boldsymbol{\Phi}_{\omega_{-n},-\boldsymbol{k}}, \tag{4}$$

$$S_4[\boldsymbol{\Phi}] = \frac{g}{\beta^4}\int \frac{d^3k_1}{(2\pi)^3}\cdots\frac{d^3k_4}{(2\pi)^3}\sum_{n_1\cdots n_4}\delta(\boldsymbol{k}_1+\boldsymbol{k}_2+\boldsymbol{k}_3+\boldsymbol{k}_4)\,\delta_{n_1+n_2+n_3+n_4}(\boldsymbol{\Phi}_{\omega_{n_1},\boldsymbol{k}_1}\cdot\boldsymbol{\Phi}_{\omega_{n_2},\boldsymbol{k}_2})(\boldsymbol{\Phi}_{\omega_{n_3},\boldsymbol{k}_3}\cdot\boldsymbol{\Phi}_{\omega_{n_4},\boldsymbol{k}_4}). \tag{5}$$

Here $\beta=1/k_BT$ and $\omega_n=2\pi n/\beta$ is a Matsubara frequency and $\boldsymbol{k}$ is measured again from the ordering wave vector. The coefficients of $\boldsymbol{k}^2$ and $|\omega_n|\cos\theta$ are made to be unity by an appropriate choice of the bare length scale ξ_0 and the temperature and energy scale T_0. In general the prefactors of the k^2 and $|\omega|$ terms for Φ_z and $\Phi_{x/y}$ will be different (even after rescaling); we suppress these prefactors to keep the notations simple as they will not lead to any qualitative changes in the results. It is, however, essential to keep track of the dynamics of $\Phi_{x/y}$, i.e., of the ratio of the precession and damping terms parametrized by an angle θ. For small θ the dynamics is overdamped, while for $\theta\sim\pi/2$ precession dominates. The value of θ depends on the details of the band structure and the size of the magnetic field, with $\theta\propto B$ for small magnetic fields.

As anticipated in (3), the x and y directions are coupled for $\theta>0$. The Gaussian part of the action can be diagonalized by introducing the complex field $\Phi^\perp\equiv(\Phi_x+\mathrm{i}\Phi_y)/\sqrt{2}$ as above, and we obtain

$$S_2[\Phi^\perp,\Phi^z] = \int\frac{d^3k}{(2\pi)^3}\frac{1}{\beta}\sum_n \Phi^{\perp}_{\omega_n,\boldsymbol{k}}{}^*[2\chi_{\boldsymbol{k}}(\mathrm{i}\omega_n)^{-1}]\Phi^\perp_{\omega_n,\boldsymbol{k}} + \Phi^z_{\omega_n,\boldsymbol{k}}(k^2+r_z+|\omega_n|)\Phi^z_{-\omega_n,-\boldsymbol{k}}, \tag{6}$$

where

$$\chi_{\boldsymbol{k}}(\mathrm{i}\omega_n)\equiv(k^2+r_\perp+|\omega_n|\cos\theta-\mathrm{i}\omega_n\sin\theta)^{-1} \tag{7}$$

is the propagator of $\Phi^\perp$.

As expected from the symmetry arguments given above, $r_\perp$ and r_z turn out to be different, with $r_z>r_\perp$ and $r_z-r_\perp \propto B^2$ for small B. As $r_{z/\perp}$ increases for increasing fields $[r(B)\approx r(0)+cB^2$ for small $B]$, an antiferromagnetic system sufficiently close to its quantum critical point can be tuned to the paramagnetic phase by applying a magnetic field (assuming that no first-order transition is induced).

When discussing the behavior close to the quantum critical point, it is important to note that the magnetic field enters into the calculations both by the B dependence of r as well as through the B-dependent angle θ. Close to the quantum critical point tuned by a *finite* magnetic field B_c, $\theta(B)\approx\theta(B_c)$ can be approximated by a constant (as checked below), while it is obviously essential to keep track of the leading B dependence of the control parameter $r(B)\propto B-B_c$.

At this point, it is worthwhile to take a closer look at $S_2[\Phi^\perp]$ in coordinate and time space for $\theta=\pi/2$, i.e., if Landau damping is absent, as it is the case in an insulator such as $TlCuCl_3$, (Ref. 9), or in a metal with $Q>2k_F$ (see the Introduction). The Gaussian part of $S_2[\Phi^\perp]$ is minimized for a field $\Phi^\perp$ that obeys the equation,

$$\mathrm{i}\partial_t\Phi^\perp = H\Phi^\perp,\quad H=(-\boldsymbol{\nabla}^2+r_\perp). \tag{8}$$

This has the form of a Schrödinger equation for a particle in a constant potential given by $V=r_\perp$. If one adds the interactions one obtains a nonlinear Schrödinger equation or Gross-Pitaevskii equation that describes the physics of weakly interacting Bosons. In this interpretation, r takes over the role of the chemical potential. The quantum critical point of a field-tuned insulating antiferromagnet ($\theta=\pi/2$) is therefore in the same universality class as the quantum phase transition of a dilute gas of Bosons driven by a chemical potential. The nonmagnetic phase ($r>0$) corresponds to a phase with *negative* chemical potential where no Bosons are present in the $T\to0$ limit, while the Bose-Einstein condensed phase (BEC) corresponds to the magnetically ordered phase.

II. RENORMALIZATION GROUP EQUATIONS AND CORRELATION LENGTH

The physical properties of the effective action (4) can be analyzed with the help of renormalization group equations. As a first step it is useful to perform a simple scaling analysis of $S[\boldsymbol{\Phi}]$. When momenta, frequencies, and fields are rescaled as $k'=kb$, $\omega'=\omega b^z$, where z is the dynamical critical exponent, and $\Phi'=\Phi b^{-(d+z+2)/2}$, $S[\boldsymbol{\Phi}]$ remains invariant under scaling, provided that $z=2$. The masses $r^{\perp,z}$ and the dimensionless coupling constant $u\equiv g\xi_0^d/T_0$ have the scaling dimensions 2 and $4-(d+z)$, respectively. In an antiferromagnetic metal, damping as well as precession are linear in frequency, and the terms therefore behave in the same way under scaling. In renormalization group terminology this implies that the precession term is an "exactly marginal" perturbation with respect to the Hertz fix point ($\theta=0, u=0$), which can be expected to modify the behavior of the system at the quantum critical point.

The renormalization group equations for the parameters T, r, and u with corrections to scaling can be obtained by closely following the procedure employed by Millis.[15] We introduce a UV cutoff in the linked cluster expansion of the free energy and express changes of that cutoff in terms of changes of the parameters of the model. The renormalization group (RG) equations are as follows:

$$\frac{\partial \mathcal{T}(b)}{\partial \log b} = z\mathcal{T}(b), \tag{9}$$

$$\frac{\partial r_\perp(b)}{\partial \log b} = 2r_\perp(b) + 4u(b)\{2f_2^\perp[r_\perp(b),\mathcal{T}(b)] + f_2^z[r_z(b),\mathcal{T}(b)]\}, \tag{10}$$

$$\frac{\partial r_z(b)}{\partial \log b} = 2r_z(b) + 4u(b)\{f_2^\perp[r_\perp(b),\mathcal{T}(b)] + 3f_2^z[r_z(b),\mathcal{T}(b)]\}, \tag{11}$$

$$\frac{\partial u(b)}{\partial \log b} = [4-(d+z)]u(b), \tag{12}$$

where $\mathcal{T}$ is the running temperature, and the expressions for $f_2^{\perp,z}$ as well as the details of the calculation can be found in Appendix B. Since the scaling dimension for u is negative for an antiferromagnetic system in three spatial dimensions, we only consider contributions up to and including the first order in u. To this order, the scaling law for u remains unmodified, and θ remains unrenormalized. The parameter θ obtains, however, finite corrections by higher-order contributions.

Equations (9) and (12) are solved trivially. As $r_z(b) > r_\perp(b)$, Φ_z remains massive at the quantum critical point ($r_z>0$ for $r_\perp=0$). In the following we will concentrate on the regime $T<r_z$, where the influence of the parallel mode Φ_z can be absorbed in a redefinition of the bare $r_\perp$.

Equation (10) can be solved for low temperatures in the limits $r_\perp/T \ll 1$ and $r_\perp/T \gg 1$, corresponding to the quantum-critical and (renormalized) Fermi-liquid regimes, respectively (see Fig. 1). This provides us with an expression for the correlation length $\xi_\perp$. We refer to Appendix B for the details of the calculation. In the quantum-critical regime $\xi_\perp^{-2}$ is given by

$$\xi_\perp^{-2}(r_\perp \ll T) = r_\perp + 16\sqrt{2}\pi^{3/2}\zeta(3/2)uT^{3/2}\cos(\theta/2), \tag{13}$$

and in the Fermi-liquid regime it has the form,

$$\xi_\perp^{-2}(T \ll r_\perp) = r_\perp + \frac{16}{3}\pi^3 uT^2 r_\perp^{1/2}\cos\theta. \tag{14}$$

For all $\theta<\pi/2$ one obtains the same qualitative behavior as in the case of the vanishing, external magnetic field.[15] Only in the Fermi-liquid regime for $\theta=\pi/2$, the T^2 correction is suppressed, as Landau damping is absent in this limit, and our model is characterized by an energy gap that leads to an exponential dependence $\exp(-r_\perp/T)$ of the correlation length.

III. THERMODYNAMIC QUANTITIES

In this section we calculate the specific heat γ, the temperature dependence of the magnetization, the magnetocaloric effect Γ_B, and the susceptibility. The free energy can be calculated directly from RG equations, again following Ref. 15. However, as the quartic coupling u is irrelevant, the leading behavior in the paramagnetic phase can equivalently be extracted just from the Gaussian free energy,

$$\begin{aligned}\mathcal{F} &\equiv \frac{\xi_0^3}{T_0 V}[F - F(T=0)] \\ &= -\frac{1}{4}\int \frac{d^3k}{(2\pi)^3}\int \frac{d\omega}{\pi}\left[\coth\left(\frac{\beta\omega}{2}\right) - 1\right] \\ &\quad \times \arctan\left[\frac{2(r+k^2)\omega\cos\theta}{(r+k^2)^2-\omega^2}\right],\end{aligned} \tag{15}$$

measured in units of T_0V/ξ_0^3, and we have set $r\equiv r_\perp$.

In Eq. (15) and in the results shown below we ignore contributions from the massive, noncritical mode Φ_z, characterized by a finite mass r_z. To the leading order, the corresponding (analytic) corrections to the free energy and its derivative are just additive and can be obtained by replacing r by r_z, by setting $\theta=0$ and by dividing the result by a factor of 2 (as there are two modes perpendicular to B) in all the formulas for thermodynamic quantities given below.

A. Specific heat

We first consider the specific-heat coefficient $c/T = \gamma(T,r) = -\partial^2\mathcal{F}/\partial T^2$. More precisely, we calculate $\tilde{\gamma} \equiv \gamma(T,r) - \gamma(T=0, r=0)$,

$$\tilde{\gamma} = \frac{1}{4}\int \frac{d^3k}{(2\pi)^3}\int \frac{dx}{\pi}\frac{2x}{e^x-1}\left(\frac{(k^2+r)^3\{4(k^2+r)^2[(k^2+r)^2+2T^2x^2]\cos\theta + 4T^4x^4\cos(3\theta)\}}{[(k^2+r)^4 + T^4x^4 + 2(k^2+r)^2T^2x^2\cos(2\theta)]^2} - \frac{4\cos\theta}{k^2}\right). \tag{16}$$

This differs from the physical specific heat by a T-independent (but cutoff-dependent) constant $\gamma_c\cos\theta$.

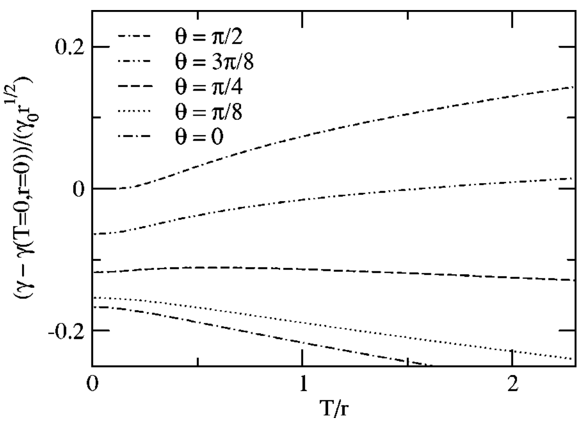

FIG. 2. Scaling function for the specific-heat coefficient $(1/\sqrt{r})\tilde{\gamma}$, where a noncritical contribution has been subtracted, $\tilde{\gamma} = \gamma(T,r) - \gamma(T=0,r=0)$. The function is not completely universal, but it depends on the parameter θ. A crossover from $\tilde{\gamma} \propto \pm T^2$ for $T \ll r$ to $\tilde{\gamma} \sim \pm\sqrt{T}$ for $r \ll T$ can be observed, where the signs depend on the value of θ. $\tilde{\gamma}(T)$ shows a maximum for $\pi/6 < \theta < \pi/3$, as can be seen more clearly in Fig. 3.

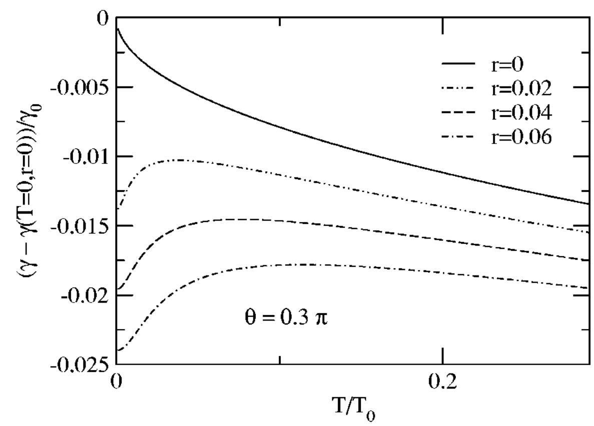

FIG. 3. Specific-heat coefficient as a function of temperature for $\theta = 0.3\pi$ and different values of r. Note that the total specific-heat coefficient γ is always positive. The maximum for $r > 0$ is characteristic for systems with $\pi/6 < \theta < \pi/3$.

The integrals can be evaluated exactly in certain limits. For $\theta = \pi/2$ and low $T \ll r$ the specific heat shows thermally activated behavior,

$$\gamma(\theta = \pi/2, T \to 0) = \frac{\sqrt{\pi}}{(2\pi)^3} \frac{r^2}{T^{3/2}} \exp\left[-\frac{r}{T}\right], \qquad (17)$$

as can be expected from a system with a gapped spectrum. For $r \ll T$ and $T \ll r$, i.e., in the quantum-critical and Fermi-liquid regimes, respectively, we obtain for $\theta < \pi/2$,

$$\tilde{\gamma}(r \ll T) = -\frac{15\sqrt{2\pi}}{32\pi^2} \zeta\left(\frac{5}{2}\right) T^{1/2} \cos\left(\frac{3}{2}\theta\right), \qquad (18)$$

$$\tilde{\gamma}(T \ll r) = -\frac{1}{6} r^{1/2} \cos\theta - \frac{\pi^2}{60} \frac{T^2}{r^{3/2}} \cos(3\theta). \qquad (19)$$

For $\theta = 0$, this reproduces well-known results[15] (correcting some factors of 2), and as expected from scaling, exponents do not change in the presence of the precession term. However, not only the sizes of the prefactors, but, interestingly, also their signs change when the dynamics begins to be dominated by precession rather than by damping. In the quantum-critical regime the $\sqrt{T}$ correction is *negative* for $\theta < \pi/3$ and positive for $\theta > \pi/3$. Also in the Fermi-liquid regime a sign change can be observed in the $T^2/r^{3/2}$ contribution at $\theta = \pi/6$.

In Fig. 2 we show the scaling function $[\tilde{\gamma}(T,r)/\sqrt{r}] = f_\theta(T/r)$ obtained from a numerical integration of (16). Due to the presence of an exactly marginal perturbation, the scaling function is *not* completely universal, but it depends on the parameter θ. In an intermediate regime, $\pi/6 < \theta < \pi/3$, $\gamma(T,r)$ [and the universal scaling function $\tilde{\gamma}(T,r)/\sqrt{r}$] shows a characteristic maximum as a function of temperature, as can be read from the asymptotical results (18) and (19). This maximum cannot be seen directly at the quantum critical point ($r=0$), but can be seen at any finite $r > 0$, as long as the critical corrections to the specific heat dominate the noncritical ones.

B. Magnetization, magnetocaloric effect, and the Grüneisen parameter

As was argued in Ref. 25, the specific heat is not the most sensitive thermodynamic quantity close to a quantum critical point, as it tracks only the variations of the free energy with respect to temperature (vertical axis in Fig. 1), but *not* with respect to the control parameter B (horizontal axis). It is therefore interesting to study also the magnetization $M = -\partial F/\partial B$, the susceptibility $\chi = -\partial^2 F/\partial B^2$, and the T derivative of M, $\partial M/\partial T = -\partial^2 F/(\partial B \partial T) = -\partial S/\partial B$. This mixed derivative has the advantage that—opposite of the specific-heat coefficient and susceptibility—it vanishes in the $T \to 0$ limit, due to the second law of thermodynamics. Therefore it is not necessary to subtract any constant noncritical contributions when measuring $\partial M/\partial T$.

Very interesting are also the ratios of the thermodynamic derivatives.[25] For a field-tuned critical point, one interesting combination is

$$\Gamma_B = -\frac{(\partial M/\partial T)_B}{T\gamma} = -\frac{1}{T}\frac{(\partial S/\partial B)_T}{(\partial S/\partial T)_B} = \left.\frac{1}{T}\frac{\partial T}{\partial B}\right|_S, \qquad (20)$$

which describes the magnetocaloric effect, i.e., the temperature change in the sample, after an adiabatic change of the magnetic field.

For pressure-tuned quantum phase transitions, where $\partial/\partial B$ is replaced by $\partial/\partial p$, the quantities related to $\partial M/\partial T$, χ and Γ_B, are the thermal expansion, the compressibility (and therefore also the sound velocity), and the Grüneisen parameter.[25]

As both control parameter r and θ depend on B, one can expect two independent critical contributions to $\partial M/\partial T$,

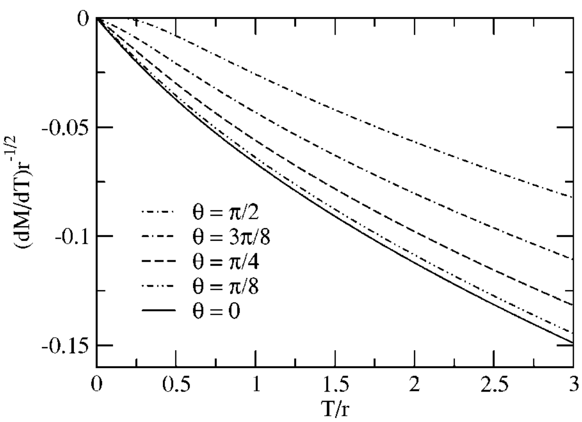

FIG. 4. Scaling function $(1/\sqrt{r})(\partial M/\partial T)$. While for the specific heat shown in Fig. 3 it was necessary to subtract a noncritical constant contribution, such a background does not exist for $\partial M/\partial T$.

$$\begin{aligned}\frac{\partial M}{\partial T} &= -\frac{\partial^2 \mathcal{F}}{\partial T \partial r}\frac{\partial r}{\partial B} - \frac{\partial^2 \mathcal{F}}{\partial T \partial \theta}\frac{\partial \theta}{\partial B} \\ &= \frac{1}{4}\int \frac{d^3k}{(2\pi)^3}\int \frac{d\omega}{\pi}\left(\frac{2e^{\omega/(2T)}}{e^{\omega/T}-1}\right)^2 \frac{\omega^2}{T^2} \\ &\quad\times\left\{\frac{[(k^2+r)^2+\omega^2]\cos\theta}{(k^2+r)^4+\omega^4+2(k^2+r)^2\omega^2\cos(2\theta)}\frac{\partial r}{\partial B}\right. \\ &\quad\left.+\frac{(k^2+r)^2[(k^2+r)^2-\omega^2]\sin\theta}{[(k^2+r)^2-\omega^2]^2+4(k^2+r)^2\omega^2\cos^2(\theta)}\frac{\partial\theta}{\partial B}\right\}.\end{aligned} \tag{21}$$

In the limits $r, T \to 0$ we obtain

$$\begin{aligned}\left.\frac{\partial M}{\partial T}\right|_{r\ll T} &= -\frac{3\sqrt{2\pi}}{16\pi^2}\zeta\left(\frac{3}{2}\right)\sqrt{T}\cos\left(\frac{\theta}{2}\right)\frac{\partial r}{\partial B} \\ &\quad -\frac{15\sqrt{2\pi}}{32\pi^2}\zeta\left(\frac{5}{2}\right)T^{3/2}\sin\left(\frac{3}{2}\theta\right)\frac{\partial\theta}{\partial B},\end{aligned} \tag{22}$$

$$\left.\frac{\partial M}{\partial T}\right|_{T\ll r} = -\frac{1}{12}\frac{T}{\sqrt{r}}\cos\theta\frac{\partial r}{\partial B} - \frac{1}{6}\sqrt{r}T\sin\theta\frac{\partial\theta}{\partial B}. \tag{23}$$

As r is a *relevant* perturbation at the quantum critical point, while θ is only *marginal*, the contributions due to the B dependence of θ are subleading and can therefore be neglected.

With $r \propto B - B_c$, we therefore find

$$\left.\frac{\partial M}{\partial T}\right|_{r\ll T} \propto -\sqrt{T}\cos\left(\frac{\theta}{2}\right), \tag{24}$$

$$\left.\frac{\partial M}{\partial T}\right|_{T\ll r} \propto -\frac{T}{\sqrt{B-B_c}}\cos\theta. \tag{25}$$

Neither $(\partial M/\partial T)_{r\ll T}$ nor $(\partial M/\partial T)_{T\ll r}$ changes sign as a function of θ, and indeed $(\partial M/\partial T)_{T,r}$ is a monotonous function of T for all values of θ (see Fig. 4).

For $\theta=\pi/2$ and at low T, the temperature derivative of the magnetization also shows thermally activated behavior,

$$\left.\frac{\partial M}{\partial T}\right|_{\theta=\pi/2, T\to 0} = -\frac{\sqrt{\pi}}{(2\pi)^3}\frac{r}{\sqrt{T}}\exp\left[-\frac{r}{T}\right]\frac{\partial r}{\partial B}. \tag{26}$$

Finally, we evaluate the magnetocaloric effect,

$$\Gamma_B = -\frac{(\partial M/\partial T)_B}{T(\tilde{\gamma}+\gamma_c\cos\theta)}, \tag{27}$$

which is given by

$$\Gamma_B(r\ll T) = \frac{6\sqrt{2}\cos\left(\frac{\theta}{2}\right)\zeta\left(\frac{3}{2}\right)}{15\sqrt{2}T\cos\left(\frac{3}{2}\theta\right)\zeta\left(\frac{5}{2}\right) - 32\sqrt{T\pi^3}\gamma_c\cos\theta}, \tag{28}$$

$$\Gamma_B(T\ll r) = \frac{1}{2(r-6\gamma_c\sqrt{r})}, \tag{29}$$

in the limits $r, T\to 0$. Due to the noncritical contribution γ_c, the result for $T\to 0$ is *not* fully universal.[25]

C. Susceptibility

Since $r\sim B-B_c$ and T have the same scaling exponents, one might expect that the susceptibility $\chi=\partial M/\partial B=-\partial^2 F/\partial B^2$ and the specific-heat coefficient $\gamma=-\partial^2 F/\partial T^2$ show very similar behavior. This, however, turns out to be *not* correct. The technical reason for this is that the susceptibility in the quantum-critical regime is a *singular* function of the (dangerously irrelevant) spin-spin interaction u. Practically, this implies that a measurement of the susceptibility is complementary to other thermodynamic measurements, as it is highly sensitive to a quantity that can otherwise be determined only by neutron-scattering measurements of the correlation length.

The susceptibility $\chi=-\partial^2 F/\partial B^2$ gets contributions both from the B-field dependence of θ and of r. We only consider the leading corrections due to r (see discussion above) and evaluate the quantity $\tilde{\chi}(r,T)=\chi(r,T)-\chi(r=0,T=0)$ with

$$\begin{aligned}\tilde{\chi} &= \int\frac{d^3k}{(2\pi)^3}\int\frac{d\omega}{\pi}\left[n_B(\omega)\mathrm{Im}\frac{1}{(k^2+r+\mathrm{i}\omega\cos\theta-\omega\sin\theta)^2}\right. \\ &\quad\left.+\Theta(-\omega)\mathrm{Im}\frac{1}{(k^2+\mathrm{i}\omega\cos\theta-\omega\sin\theta)^2}\right].\end{aligned} \tag{30}$$

Most interesting is the quantum-critical regime, where the leading correction to the susceptibility takes the form,

$$\tilde{\chi}(r\ll T) \approx \left[\frac{1}{8\pi}\frac{T}{\sqrt{r}} - \frac{\sqrt{2}}{4\pi^2}\sqrt{T}\cos\left(\frac{\theta}{2}\right)\right]\left(\frac{\partial r}{\partial B}\right)^2. \tag{31}$$

Note that this expression formally *diverges* for $r\to 0$. This implies that we have to take into account the interaction effects discussed in Sec. II, and we have to replace the control parameter r by $\xi_\perp^{-2}(T)\sim r+uT^{3/2}$, given by Eq. (13). One therefore finds

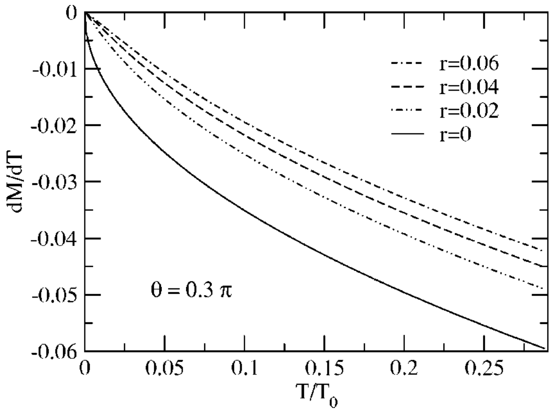

FIG. 5. $\partial M/\partial T$ as a function of temperature for $\theta=0.3\pi$ and different values of r. At the quantum critical point we obtain $\partial M/\partial T \sim -\sqrt{T}$ while $\partial M/\partial T \sim -T/\sqrt{r}$ for $T \ll r$.

$$\tilde{\chi} \propto \frac{T}{\sqrt{r}} \quad \text{for} \quad r < T < (r/u)^{2/3}, \tag{32}$$

but

$$\tilde{\chi} \propto \frac{T^{1/4}}{\sqrt{u}} \quad \text{for} \quad T > (r/u)^{2/3}. \tag{33}$$

Scaling is violated, i.e., the susceptibility is no longer of the form $\tilde{\chi}(r,T)=f_\theta(T/r)/\sqrt{r}$, as the dangerously irrelevant coupling u determines $\tilde{\chi}$ in this regime. It is interesting to trace the origin of the $1/\sqrt{r}$ contribution in (31). It arises from the $\omega_n=0$ mode of the Gaussian theory (6), which leads to a contribution of the form $T\Sigma_k 1/(k^2+r)^2$ to the susceptibility. Note that the static $\omega=0$ contribution does not depend on the dynamics; i.e., it does not depend on θ. However, the correlation length $\xi_\perp(T)$ given in Eq. (13) does depend smoothly on θ, which leads to a slight θ dependence of $\tilde{\chi}$.

In the Fermi-liquid regime, the susceptibility is given by

$$\tilde{\chi}(T \ll r) = \left(-\frac{1}{4\pi^2}\sqrt{r}\cos\theta + \frac{1}{48}\frac{T^2}{r^{3/2}}\cos\theta\right)\left(\frac{\partial r}{\partial B}\right)^2, \tag{34}$$

while for $\theta=\pi/2$ and low $T \ll r$ it shows thermally activated behavior,

$$\chi(\theta=\pi/2, T\to 0) = \left(\frac{\sqrt{\pi}}{(2\pi)^3}\sqrt{T}\exp\left[-\frac{r}{T}\right]\right)\left(\frac{\partial r}{\partial B}\right)^2. \tag{35}$$

The rapid crossovers between the T^2, T, and $T^{1/4}$ regimes are shown in Fig. 5.

IV. SCATTERING RATE

Due to energy and momentum conservation, the scattering of electrons from spin fluctuations is most efficient close to "hot lines" on the Fermi surface, where $E_{\boldsymbol{k}}=E_{\boldsymbol{k}\pm\boldsymbol{Q}}=0$ and $\boldsymbol{Q}$ is the ordering vector of the antiferromagnet. In order to determine how spin precession modifies the results we calculate the scattering rate as a function of θ. We will neglect all orbital effects of the magnetic field and will not try to calculate the conductivity and the Hall effect. For an extensive discussion of orbital effects and magnetotransport in nearly antiferromagnetic metals see Ref. 24, which does not consider, however, the effects of spin precession.

In second-order perturbation theory the lifetime of the spin-up electron scattering from fluctuations of $\Phi_\perp$ at $T=0$ is given by[26]

$$\frac{1}{\tau_{\boldsymbol{k}}^{\uparrow}} = 2g_s^2\sum_{\boldsymbol{k}'}\int_0^{\epsilon_{\boldsymbol{k}}} d\omega\, \mathrm{Im}\,\chi_{\boldsymbol{k}-\boldsymbol{k}'}(\omega)\,\delta[\omega-(E_{\boldsymbol{k}}^{+}-E_{\boldsymbol{k}'}^{-})], \tag{36}$$

where g_s is a coupling constant, $E_{\boldsymbol{k}}^{+/-}$ and $v_F^{+/-}$ are the energy and velocity of spin-up and spin-down electrons, and χ is the spin-fluctuation spectrum of Eq. (7),

$$\chi_{\boldsymbol{q}}(\omega) = \frac{1}{\omega_{\boldsymbol{q}} + r + \mathrm{i}\omega\cos\theta - \omega\sin\theta}, \tag{37}$$

with $\omega_{\boldsymbol{q}}=(\boldsymbol{q}\pm\boldsymbol{Q})^2/q_0^2$. We split the momentum integration in an integral over the Fermi surface and an energy integration $\int d^3\boldsymbol{k}' = \int\int d\boldsymbol{k}'/v_F^- \int dE_{k'}^-$ and integrate first over $E_{k'}^-$ and then over ω to obtain

$$\begin{aligned}\frac{1}{\tau_{\boldsymbol{k}}^{\uparrow}} \approx{}& \frac{g_s^2}{v_F^-(2\pi)^3}\int\int d\boldsymbol{k}' \\ &\times\left(\cos\theta\ln\left[\frac{(\omega_{\boldsymbol{k}-\boldsymbol{k}'}+r)^2 + 2E_{\boldsymbol{k}}^+\sin\theta + (E_{\boldsymbol{k}}^+)^2}{(\omega_{\boldsymbol{k}-\boldsymbol{k}'}+r)^2}\right]\right. \\ &\left. + \sin\theta\arctan\left[\frac{-E_{\boldsymbol{k}}^+\cos\theta}{\omega_{\boldsymbol{k}-\boldsymbol{k}'}+r+E_{\boldsymbol{k}}^+\sin\theta}\right]\right)\end{aligned} \tag{38}$$

$$\approx \frac{g_s^2 q_0^2}{v_F^-(2\pi)^2}E_{\boldsymbol{k}}^+ \min\left\{\frac{E_{\boldsymbol{k}}^+}{2\delta_k^2}\cos\theta, \frac{\pi}{2}-\theta\right\}, \tag{39}$$

where $\delta_k = r + (\delta\boldsymbol{k}/q_0)^2$ and $\delta\boldsymbol{k}$ is the distance of $\boldsymbol{k}+\boldsymbol{Q}$ from the Fermi surface or, approximately, the distance of $\boldsymbol{k}$ from hot lines on the Fermi surface. Analogously we obtain for spin-down electrons

$$\frac{1}{\tau_{\boldsymbol{k}}^{\downarrow}} \approx \frac{g_s^2 q_0^2}{v_F^+(2\pi)^2}E_{\boldsymbol{k}}^- \min\left\{\frac{E_{\boldsymbol{k}}^-}{2\delta_k^2}\cos\theta, \frac{\pi}{2}-\theta\right\}, \tag{40}$$

where the indices + and − have been exchanged with respect to Eq. (38). The scattering rate is strongly dependent on the distance from the hot lines; at the quantum critical point and for $\delta\boldsymbol{k}/q_0 \approx 0$ the scattering rate is linear in the quasiparticle energy. Far away from the hot lines and the quantum critical point the usual scattering rate $1/\tau_{\boldsymbol{k}}^{\uparrow,\downarrow} \propto E_{\boldsymbol{k}}^{+,-2}$ is recovered.[24] The main result of this section is that the spin-precession term does not lead to a qualitative change in the scattering rate.

V. DISCUSSION

In this paper, we discussed the field-induced quantum phase transition of a clean, three-dimensional antiferromag-

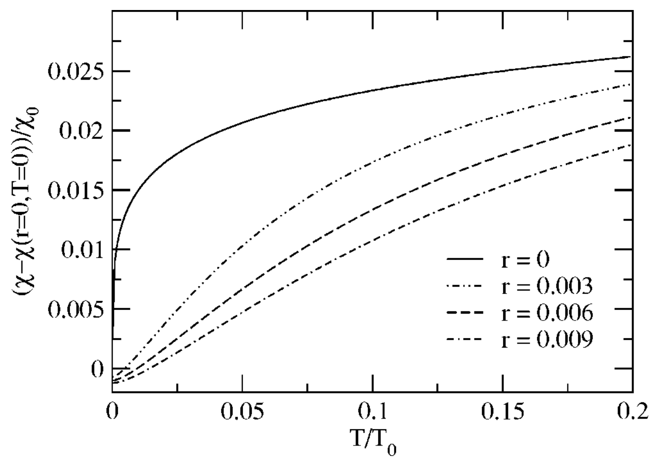

FIG. 6. Susceptibility as a function of temperature for $u=0.2$, $\theta=0.01$, and different values of r. Curves for other values of θ look essentially identical and are not shown. Note that the susceptibility is *much more* sensitive to small deviations from the quantum critical point than the specific-heat coefficient or $\partial M/\partial T$ (c.f. Figs. 3 and 6 where much larger values for r have been used). The $T^{1/4}$ cusp at the quantum critical point [Eq. (33)] is rapidly washed out by tiny deviations from the critical magnetic field and replaced by the linear dependence of Eq. (32).

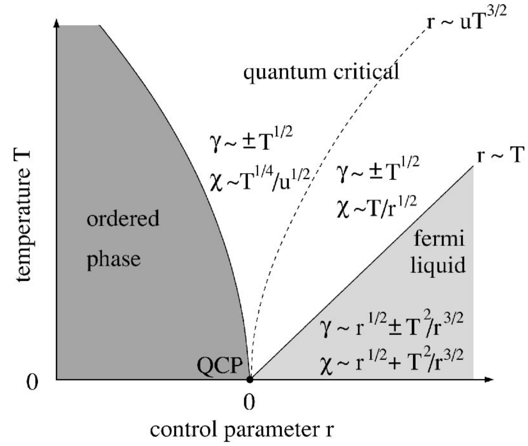

FIG. 7. Qualitative behavior of specific-heat coefficient γ and magnetic susceptibility χ in various regimes of the phase diagram.

netic metal, restricting our attention to the nonmagnetic side of the phase diagram. The main question was how the interplay of the precession of the spins in the presence of a finite magnetic field and Landau damping modifies the quantum critical behavior.

One main qualitative result of our analysis is that the critical behavior is *not* completely universal, as it depends on a continuous variable θ that parametrizes the ratio of the precession and damping terms in the effective action. While critical exponents do not depend on θ, this parameter strongly changes the scaling functions and even the sign of leading corrections, e.g., to the specific heat.

A requirement for the validity of our analysis is that the two modes $\Phi_{x,y}$ perpendicular to the magnetic field are characterized by the same mass. In the presence of sizable spin-orbit couplings, this will be the case only if the crystal has a sufficiently high symmetry and if, furthermore, the external magnetic field is applied along the symmetry direction of a crystal.

Presently, we are not aware of any experiments that show, for example, the maximum in the T dependence of the specific-heat coefficient that we predict for $\pi/6<\theta<\pi/3$. Note that in systems such as $CeCu_{5.2}Ag_{0.8}$ (Ref. 1) or $CeCu_{3.8}Au_{0.2}$ (Ref. 2) strong anisotropies prohibit the precession of the spin, i.e., $\theta=0$. Under what conditions can large values of θ be expected? Obviously, large uniform magnetizations are required. In heavy Fermion systems with Kondo temperatures of the order of a few Kelvin, one can introduce strong magnetic polarizations with moderate external fields, and it should therefore be possible to induce sizable values of θ. A different class of systems which might be of interest in this context are ferromagnetic materials. If it is possible to suppress only the staggered component of the magnetization in such systems, either by external fields, pressure, or doping, the critical theory within the Hertz approach will be characterized by a finite (and again sizable) θ.

As long as the ordering vector $\boldsymbol{Q}$ of the antiferromagnet can connect the spin-up and spin-down Fermi surfaces ($Q<k_F^+ + k_F^-$ or, more precisely, $E_{\boldsymbol{k}}^+ = E_{\boldsymbol{k}\pm\boldsymbol{Q}}^- = 0$ for a line of momenta $\boldsymbol{k}$), Landau damping is present and $\theta<\pi/2$. In contrast, one finds $\theta=\pi/2$ in all systems where no such connection exists ($Q>k_F^+ + k_F^-$). However, the transition from $\theta<\pi/2$ to $\theta=\pi/2$ is *not* expected to be smooth, as the interactions of the spin fluctuations diverge and become relevant[15,27] at the point where $Q=k_F^+ + k_F^-$.

According to our analysis, the susceptibility $\partial M/\partial B$ is a particularly interesting experimental quantity to study close to a field-driven quantum critical point. First of all, it is expected to be much more sensitive to small deviations from criticality, compared to changes in other thermodynamic quantities (see Fig. 5). Second, it allows us to measure the correlation length, a quantity that cannot be extracted from other thermodynamic quantities, as for $B=B_c$ we obtain from (31),

$$\frac{\chi(T)-\chi(T=0)}{T} \propto \xi(T). \tag{41}$$

Third, it strongly violates $T/(B-B_c)$ scaling. This deviation from scaling for χ can be used to show that the relevant critical theory is above its upper critical dimension, a central question for the interpretation of quantum criticality in systems such as $CeCu_{6-x}Au_x$ or $YbRh_2Si_2$.[2,4] All of these three statements are actually independent of the value of θ; they apply equally for a dynamics that is overdamped, $\theta\ll 1$, or for a BEC system such as $TlCuCl_3$ with $\theta=\pi/2$. Note that in pressure-tuned quantum critical points the compressibility κ (and therefore the sound velocity[28]) plays the same role as χ for field-tuned quantum phase transitions. An overview of the qualitative T dependence of the specific heat and susceptibility is shown in Fig. 7.

Field-tuned quantum phase transitions in metals allow us to study quantum critical behavior with a tuning parameter that can easily be controlled and with a conjugate field—the uniform magnetization—that can be directly measured. They are therefore especially well suited to answer some of the central questions in the field of quantum-critical metals, for example, whether or not such systems can be described in terms of simple spin-fluctuation theories, such as those that have been used in this paper.

ACKNOWLEDGMENTS

We thank T. Lorenz, B. Luethi, S. Paschen, A. Schofield, N. Shah, Q. Si, and M. Vojta for useful discussions and the Emmy-Noether program and SFB 608 of the DFG for financial support.

APPENDIX A: CUBIC TERMS IN THE EFFECTIVE ACTION

In this appendix we briefly discuss whether cubic terms Φ^3 are present in the low-energy, effective Lagrangian. As Φ carries the momentum $\boldsymbol{Q}$, the presence of such terms is forbidden by momentum conservation in most systems, with the exception of magnetic structures [e.g., body-centered cubic (bcc) lattices], where the sum of the three ordering vectors adds up to 0. If such a system has Ising symmetry, then a cubic term does exist and the magnetic-field-driven transition will be first order. However, for *xy* symmetry perpendicular to the magnetic field (the case mostly discussed in this paper), a rotationally invariant cubic term of the form $\Phi_\perp^3$ does *not* exist. While terms such as $B\Phi_z|\Phi_\perp|^2$ *are* allowed by symmetry, they lead effectively only to a renormalization of the $|\Phi_\perp|^4$ interaction as Φ_z remains massive. We therefore neglect such terms.

APPENDIX B: DERIVATION OF RG EQUATIONS

Following Millis' treatment,[15,29] we perform the renormalization-group analysis on the free energy after having converted all Matsubara sums to integrals. Although we restrict our calculations to systems in three spatial dimensions and with a dynamical critical exponent of $z=2$, we nonetheless keep the variables d and z in the calculation in order to make the origin of certain factors more transparent.

The free energy can be obtained via a linked cluster expansion in the coupling constant u. The scaling dimension of u is $4-(d+z)$, which is negative for an antiferromagnetic system in three spatial dimensions. To the first order in u, only the diagram in Fig. 8 contributes to the free energy. Up to the first order in u, the free energy $\mathcal{F}$ is therefore given by

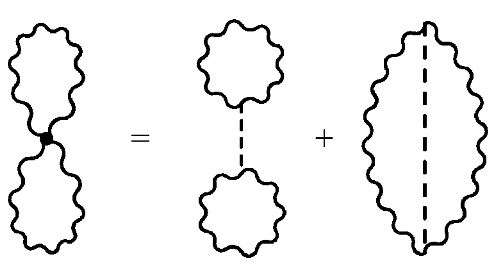

FIG. 8. Diagram contributing to the free energy in $\mathcal{O}(u)$. The different contractions of the internal indices of the fields involved have been made explicit on the right hand side, where the dashed line represents the quartic interaction u.

$$\mathcal{F} = \mathcal{F}_G + u[(I_\chi + I_{\chi^*} + I_{\chi^z})^2 + 2(I_\chi^2 + I_{\chi^*}^2 + I_{\chi^z}^2)], \quad \text{(B1)}$$

where

$$\mathcal{F}_G = -\frac{1}{2}\int_0^\Lambda \frac{d^3k}{(2\pi)^3}\int_0^\Gamma \frac{d\omega}{\pi}\coth\left(\frac{\beta\omega}{2}\right) \times \arctan\left[\frac{2(r+k^2)\omega\cos\theta}{(r+k^2)^2-\omega^2}\right] \quad \text{(B2)}$$

is the Gaussian free energy measured in units of T_0V/ξ_0^3, with the cutoffs Λ and Γ; I_χ is given by

$$I_\chi \equiv \int \frac{d^3k}{(2\pi)^3}\frac{1}{\beta}\sum_n \chi_{\boldsymbol{k}}(i\omega_n) = \int_0^\Lambda \frac{d^3k}{(2\pi)^3}\int_0^\Gamma \frac{d\omega}{\pi}\coth\left(\frac{\beta\omega}{2}\right) \times \frac{\omega\cos\theta}{(r+k^2)^2 - 2(r+k^2)\omega\sin\theta + \omega^2}, \quad \text{(B3)}$$

and I_{χ^*}, I_{χ^z} are defined analogously.

As a next step, we separate out of the momentum and frequency integrals in the expressions on the right-hand side of (B1) the regions given by $\{\Lambda \geqslant k \geqslant \Lambda/b, \Gamma \geqslant \omega \geqslant 0\}$ and $\{\Lambda \geqslant k \geqslant 0, \Gamma \geqslant \omega \geqslant \Gamma/b^2\}$. Considering that

$$I_\chi + I_{\chi^*} = 2\frac{\partial \mathcal{F}_G}{\partial r_\perp}, \quad I_{\chi^z} = 2\frac{\partial \mathcal{F}_G}{\partial r_z}, \quad \text{(B4)}$$

the change in $\mathcal{F}$ upon such a variation of the cutoff can be expressed as a change of $r_\perp$ and r_z, and this leads to the equations,

$$\frac{\partial r_\perp(b)}{\partial \log b} = 2r_\perp(b) + 4u(b)\{2f_2^\perp[r_\perp(b),\mathcal{T}(b)] + f_2^z[r_z(b),\mathcal{T}(b)]\}, \quad \text{(B5)}$$

$$\frac{\partial r_z(b)}{\partial \log b} = 2r_z(b) + 4u(b)\{f_2^\perp[r_\perp(b),\mathcal{T}(b)] + 3f_2^z[r_z(b),\mathcal{T}(b)]\}, \quad \text{(B6)}$$

for the running masses $r_\perp(b)$, $r_z(b)$, where $f_2^\perp$ and f_2^z are given by

$$f_2^\perp(r_\perp,\mathcal{T}) = K_3\Lambda^3\int_0^\Gamma \frac{d\omega}{\pi}\coth\left(\frac{\beta\omega}{2}\right) \times \frac{2\omega[(\Lambda^2+r_\perp)^2+\omega^2]\cos\theta}{[(\Lambda^2+r_\perp)^2+\omega^2]^2-4(\Lambda^2+r_\perp)^2\omega^2\sin^2\theta} + \frac{z\Gamma}{\pi}\int_0^\Lambda \frac{d^3k}{(2\pi)^3}\coth\left(\frac{\beta\Gamma}{2}\right) \times \frac{2\Gamma[(k^2+r_\perp)^2+\Gamma^2]\cos\theta}{[(k^2+r_\perp)^2+\Gamma^2]^2-4(k^2+r_\perp)^2\Gamma^2\sin^2\theta},$$

$$f_2^z(r_z,\mathcal{T}) = K_3\Lambda^3\int_0^\Gamma \frac{d\omega}{\pi}\coth\left(\frac{\beta\omega}{2}\right)\frac{\omega}{(r_z+\Lambda^2)^2+\omega^2} + \frac{z\Gamma}{\pi}\int_0^\Lambda \frac{d^3k}{(2\pi)^3}\coth\left(\frac{\beta\Gamma}{2}\right)\frac{\Gamma}{(r_z+k^2)^2+\Gamma^2}. \tag{B7}$$

In the following we assume that the system is close to the quantum critical point at temperatures much lower than r_z. In this case, $f_2^z(r_z,\mathcal{T})$ can be set to zero, and the renormalization group flow of $r_\perp$ is determined by $f_2^\perp(r_\perp,\mathcal{T})$ only. There are two contributions to $f_2^\perp$, one from the renormalization due to the separated momentum shell, where momentum is set on shell $k=\Lambda$, and one from the renormalization due to the frequency shell with $\omega=\Gamma$. For subsequent calculations we note that

$$f_2^\perp(r_\perp,\mathcal{T}) - f_2^\perp(r_\perp,0) = K_3\Lambda^3\int_0^\Gamma\frac{d\omega}{\pi}\left[\coth\left(\frac{\beta\omega}{2}\right)-1\right] \times\frac{2\omega[(\Lambda^2+r_\perp)^2+\omega^2]\cos\theta}{[(\Lambda^2+r_\perp)^2+\omega^2]^2-4(\Lambda^2+r_\perp)^2\omega^2\sin^2\theta} + \mathcal{O}(e^{-\Gamma/\mathcal{T}}). \tag{B8}$$

In other words, the contribution of the frequency shell renormalizes the zero-temperature properties only and is exponentially suppressed at finite temperatures.

In order to obtain an expression for the correlation length, we first substitute $r_\perp(b)=R_\perp(b)b^2$ to eliminate the naive scaling and then formally integrate Eq. (B5),

$$R_\perp(b) = r_0^\perp + 8\int_0^{\ln b} dx e^{-2x}u(e^x)f_2^\perp[R_\perp(e^x)e^{2x},\mathcal{T}e^{zx}]. \tag{B9}$$

We then perform an expansion in temperature,

$$R_\perp(b) \sim \Delta_\perp(b) + R_T^\perp(b) + \delta R_\perp(b), \tag{B10}$$

where three terms contribute.

The first term $\Delta_\perp(b)$ is the running mass at zero temperature,

$$\Delta_\perp(b) = r_0^\perp + 8\int_0^{\ln b} dx e^{-2x}u(e^x)f_2^\perp[\Delta_\perp(e^x)e^{2x},0]. \tag{B11}$$

The integrand can now be expanded in $\Delta_\perp$ which leads to the following expression:

$$\Delta_\perp(b) \sim r_0^\perp + 8f_2^\perp(0,0)\int_0^{\ln b} dx e^{-2x}u(e^x) \xrightarrow{b\to\infty} r_0^\perp - r_c^\perp \equiv r_\perp, \tag{B12}$$

and this defines the parameter that characterizes the distance from the critical point.

The other two terms in (B10) are of the first order in temperature. One contribution is due to an explicit dependence of $f_2^\perp$ on the running temperature,

$$R_T^\perp(b) = 8\int_0^{\ln b} dx e^{-2x}u(e^x)\{f_2^\perp[R_\perp(e^x)e^{2x},\mathcal{T}e^{zx}] - f_2^\perp[R_\perp(e^x)e^{2x},0]\}, \tag{B13}$$

and $\delta R_\perp(b)$ originates from the temperature dependence of the running mass,

$$\delta R_\perp(b) = 8\int_0^{\ln b} dx e^{-2x}u(e^x)\{f_2^\perp[R_\perp(e^x)e^{2x},0] - f_2^\perp[\Delta_\perp(e^x)e^{2x},0]\}. \tag{B14}$$

This term is of the order of u^2, and it will be neglected from now on.

The inverse square of the correlation length $\xi_\perp$ is given by

$$\xi_\perp^{-2} = \lim_{b\to\infty}\{\Delta(b)+R_T^\perp(b)\} = r_\perp + \lim_{b\to\infty} 8\int_0^{\ln b} dx e^{-2x}u(e^x)K_3\Lambda^3 \times \int_0^\Gamma \frac{d\omega}{\pi}\left[\coth\left(\frac{\omega}{2\mathcal{T}e^{zx}}\right)-1\right]\frac{2\omega\{[\Lambda^2+R_\perp(e^x)e^{2x}]^2+\omega^2\}\cos\theta}{\{[\Lambda^2+R_\perp(e^x)e^{2x}]^2+\omega^2\}^2-4[\Lambda^2+R_\perp(e^x)e^{2x}]^2\omega^2\sin^2\theta} \tag{B15}$$

$$
=r_\perp + 16\Lambda^{d+z-2}K_d T^{2/z}\int_{\ln(T^{1/z}/\Lambda)}^{\infty} dx u(e^x\Lambda T^{-1/z})e^{(z-2)x}\int_0^\infty \frac{dv}{\pi}(\coth v - 1)
$$

$$
\times\frac{4\Lambda^z e^{zx} v\{[\Lambda^2 + R_\perp(e^x\lambda T^{1/z})e^{2x}\Lambda^2 T^{-2/z}]^2 + 4\Lambda^{2z}e^{2zx}v^2\}\cos\theta}{\{[\Lambda^2 + R_\perp(e^x\lambda T^{1/z})e^{2x}\Lambda^2 T^{-2/z}]^2 + 4\Lambda^{2z}e^{2zx}v^2\}^2 - 16[\Lambda^2 + R_\perp(e^x\lambda T^{1/z})e^{2x}\Lambda^2 T^{-2/z}]^2 v^2\Lambda^{2x}e^{2zx}\sin^2\theta}, \tag{B16}
$$

where the transformations $e^x \to e^x\Lambda^{-1}T^{1/z}$ and $v=\omega/2Te^{zx}$ are introduced, and $u(e^x\Lambda T^{-1/z})=u_0(e^x\Lambda T^{-1/z})^{4-(d+z)}$. Expression (B16) for the correlation length can now be evaluated in the quantum-critical and Fermi-liquid regimes.

In the quantum-critical regime we can neglect the dependence of the integrand of (B16) on $R_\perp$ and extend the lower limit of the x integral to $-\infty$. Using the following integral:

$$
\int_0^\infty d\xi \frac{(2\xi)^n}{\sinh^2\xi} = 2n\Gamma(n)\zeta(n), \quad n=0,1,2,\ldots, \tag{B17}
$$

we obtain

$$
\xi_\perp^{-2} = r_\perp + 16\frac{K_d}{z\cos\left(\frac{d-2}{2z}\pi\right)}\Gamma\left(1+\frac{d-2}{z}\right)\zeta\left(1+\frac{d-2}{z}\right)
\times uT^{(d+z-2)/z}\cos\left(\frac{d-2}{z}\theta\right). \tag{B18}
$$

In the Fermi-liquid regime and for low temperatures, we can replace the running mass $R_\perp$ in (B16) by the control parameter $r_\perp$. It is convenient at this point to introduce yet another variable transformation of the form $e^{2x'}=r_\perp T^{-2/z}e^{2x}$. To the lowest order we can then neglect the term $Tr_\perp^{-z/2}$ in the integrand. Furthermore, we can extend the lower limit of the x integral to $-\infty$, thereby inducing an error of order $\mathcal{O}(r_\perp^{1/2}/\Lambda)^{2-d+z}$ and obtain

$$
\xi_\perp^{-2} = r_\perp + 16\frac{\pi^2}{12}\frac{d-z}{\sin\left(\frac{d-z}{2}\pi\right)}K_d uT^2 r_\perp^{(d-z-2)/2}\cos\theta \tag{B19}
$$

in the Fermi-liquid regime.

[1] K. Heuser, E.-W. Scheidt, T. Schreiner, and G. R. Stewart, Phys. Rev. B **57**, R4198 (1998); K. Heuser, E.-W. Scheidt, T. Schreiner, and G. R. Stewart, Phys. Rev. B **58**, R15 959 (1998).

[2] H. v. Löhneysen, C. Pfleiderer, T. Pietrus, O. Stockert, and B. Will, Phys. Rev. B **63**, 134411 (2001).

[3] E. Bauer, A. Galatanu, L. Naber, M. Galli, F. Marabelli, C. Seuring, K. Heuser, E.-W. Scheidt, T. Schreiner, and G. R. Stewart, Physica B **281–282**, 319 (2000).

[4] J. Custers, P. Gegenwart, H. Wilhelm, K. Neumaier, Y. Tokiwa, O. Trovarelli, C. Geibel, F. Steglich, C. Pépin, P. Coleman, Nature (London) **424**, 524 (2003); P. Gegenwart, J. Custers, C. Geibel, K. Neumaier, T. Tayama, K. Tenya, O. Trovarelli, and F. Steglich, Phys. Rev. Lett. **89**, 056402 (2002).

[5] J. S. Kim, N. O. Moreno, J. L. Sarrao, J. D. Thompson, and G. R. Stewart, Phys. Rev. B **69**, 024402 (2004).

[6] S. L. Bud'ko, E. Morosan, and P. C. Canfield, Phys. Rev. B **69**, 014415 (2004).

[7] A. Bianchi, R. Movshovich, I. Vekhter, P. G. Pagliuso, and J. L. Sarrao, Phys. Rev. Lett. **91**, 257001 (2003).

[8] J. Paglione, M. A. Tanatar, D. G. Hawthorn, E. Boaknin, R. W. Hill, F. Ronning, M. Sutherland, Louis Taillefer, C. Petrovic, and P. C. Canfield, Phys. Rev. Lett. **91**, 246405 (2003).

[9] A. Oosawa, M. Ishii, and H. Tanaka, J. Phys.: Condens. Matter **11**, 265 (1999); C. Rüegg, N. Cavadini, A. Furrer, H.-U. Güdel, K. Krämer, H. Mutka, A. Wildes, K. Habicht, and P. Vorderwisch, Nature (London) **423**, 62 (2003).

[10] H. Kageyama, K. Yoshimura, R. Stern, N. V. Mushnikov, K. Onizuka, M. Kato, K. Kosuge, C. P. Slichter, T. Goto, and Y. Ueda, Phys. Rev. Lett. **82**, 3168 (1999).

[11] M. Jaime, V. F. Correa, N. Harrison, C. D. Batista, N. Kawashima, Y. Kazuma, G. A. Jorge, R. Stern, I. Heinmaa, S. A. Zvyagin, Y. Sasago, and K. Uchinokura, Phys. Rev. Lett. **93**, 087203 (2004).

[12] S. A. Grigera, R. S. Perry, A. J. Schofield, M. Chiao, S. R. Julian, G. G. Lonzarich, S. I. Ikeda, Y. Maeno, A. J. Millis, A. P. Mackenzie, Science **294**, 329 (2001); A. J. Millis, A. J. Schofield, G. G. Lonzarich, S. A. Grigera, Phys. Rev. Lett. **88**, 217204 (2002); R. S. Perry, K. Kitagawa, S. A. Grigera, R. A. Borzi, A. P. Mackenzie, K. Ishida, and Y. Maeno, Phys. Rev. Lett. **92**, 166602 (2004).

[13] T. Moriya, *Spin Fluctuations in Itinerant Electron Magnetism* (Springer Verlag, Berlin 1985).

[14] J. A. Hertz, Phys. Rev. B **14**, 1165 (1976).

[15] A. J. Millis, Phys. Rev. B **48**, 7183 (1993).

[16] H. v. Löhneysen, T. Pietrus, G. Portisch, H. G. Schlager, A. Schröder, M. Sieck, and T. Trappmann, Phys. Rev. Lett. **72**, 3262 (1994); A. Rosch, A. Schröder, O. Stockert, and H. v. Löhneysen, Phys. Rev. Lett. **79**, 159 (1997); O. Stockert, H. v. Löhneysen, A. Rosch, N. Pyka, and M. Loewenhaupt, *ibid.* **80**, 5627 (1998); A. Schröder, G. Aeppli, R. Coldea, M. Adams, O. Stockert, H. v. Löhneysen, E. Bucher, R. Ramazasavili, and P. Coleman, Nature (London) **407**, 351 (2000).

[17] Q. Si, S. Rabello, K. Ingersent, and J. L. Smith, Nature (London) **413**, 804 (2001); T. Senthil, S. Sachdev, and M. Vojta, Phys. Rev. Lett. **90**, 216403 (2003).
[18] S. Sachdev, *Quantum Phase Transitions* (Cambridge University Press, Cambridge, 1999).
[19] I. Affleck, Phys. Rev. B **43**, 3215 (1991).
[20] T. Nikuni, M. Oshikawa, A. Oosawa, and H. Tanaka, Phys. Rev. Lett. **84**, 5868 (2000).
[21] T. Giamarchi and A. M. Tsvelik, Phys. Rev. B **59**, 11 398 (1999).
[22] M. Matsumoto, B. Normand, T. M. Rice, and M. Sigrist, Phys. Rev. Lett. **89**, 077203 (2002).
[23] O. Nohadani, S. Wessel, and S. Haas, cond-mat/0411599 (unpublished).
[24] A. Rosch, Phys. Rev. B **62**, 4945 (2000).
[25] L. Zhu, M. Garst, A. Rosch, and Q. Si, Phys. Rev. Lett. **91**, 066404 (2003).
[26] R. Hlubina and T. M. Rice, Phys. Rev. B **51**, 9253 (1995).
[27] B. L. Altshuler, L. B. Ioffe, and A. J. Millis, Phys. Rev. B **52**, 5563 (1995).
[28] We thank B. Luethi for pointing out that the sound velocity is an interesting quantity to study at a quantum critical point.
[29] M. Garst, Ph.D. thesis, Universität Karlsruhe, 2003.